

# Role of the Cytokine-induced SH2 Domain-containing Protein CIS in Growth Hormone Receptor Internalization\*

Received for publication, April 15, 2005, and in revised form, September 2, 2005. Published, JBC Papers in Press, September 8, 2005, DOI 10.1074/jbc.M504125200

Tanya Landsman and David J. Waxman<sup>1</sup>

From the Division of Cell and Molecular Biology, Department of Biology, Boston University, Boston, Massachusetts 02215

The cytokine-inducible SH2 domain-containing protein CIS inhibits signaling from the growth hormone (GH) receptor (GHR) to STAT5b by a proteasome-dependent mechanism. Here, we used the GH-responsive rat liver cell line CWSV-1 to investigate the role of CIS and the proteasome in GH-induced GHR internalization. Cell-surface GHR localization and internalization were monitored in GH-stimulated cells by confocal immunofluorescence microscopy using an antibody directed against the GHR extracellular domain. In GH naive cells, GHR was detected in small, randomly distributed granules on the cell surface and in the cytoplasm, with accumulation in the perinuclear area. GH treatment induced a rapid (within 5 min) internalization of GH·GHR complexes, which coincided with the onset of GHR tyrosine phosphorylation and the appearance in the cytosol of distinct granular structures containing internalized GH. GHR signaling to STAT5b continued for ~30–40 min, however, indicating that GHR signaling and deactivation of the GH·GHR complex both proceed from an intracellular compartment. The internalization of GH and GHR was inhibited by CIS-R107K, a dominant-negative SH2 domain mutant of CIS, and by the proteasome inhibitors MG132 and epoxomicin, which prolong GHR signaling to STAT5b. GH pulse-chase studies established that the internalized GH·GHR complexes did not recycle back to the cell surface in significant amounts under these conditions. Given the established specificity of CIS-R107K for blocking the GHR signaling inhibitory actions of CIS, but not those of other SOCS/CIS family members, these findings implicate CIS and the proteasome in the control of GHR internalization following receptor activation and suggest that CIS-dependent receptor internalization is a prerequisite for efficient termination of GHR signaling.

Growth hormone (GH)<sup>2</sup> is an important regulator of somatic growth and cellular metabolism. GH exerts its action via the GH receptor (GHR), a transmembrane protein of the cytokine receptor superfamily that activates multiple intracellular signaling pathways, including the STAT, mitogen-activated protein kinase, phosphatidylinositol 3-kinase, and protein kinase C pathways (1, 2). Upon binding of ligand, the dimeric GHR undergoes a conformational change (3, 4) and induces tyrosine phosphorylation, resulting in activation of the tyrosine kinase JAK2, which catalyzes tyrosine phosphorylation of GHR and of GHR-

JAK2-associated STAT1, STAT3, STAT5a, and STAT5b (5, 6). The tyrosine-phosphorylated STAT proteins dimerize and translocate to the nucleus, where they bind to specific DNA response elements upstream of GH target genes and activate gene transcription (7, 8).

Many physiological responses to GH are dependent on the temporal pattern of plasma GH stimulation, which is sex-dependent and subject to neuroendocrine control. In the rat model, the adult male plasma GH pattern is characterized by regular pulses of hormone every ~3.5–4 h, separated by well defined GH-free intervals, whereas a more continuous plasma GH profile is associated with adult females (9). These sex-dependent plasma GH profiles dictate the sex-dependent expression of a large number of liver gene products, including various plasma proteins, enzymes of steroid and foreign compound metabolism, receptors, and other signaling molecules (10). Targeted gene disruption studies show that the sexual dimorphism of liver gene expression in males requires STAT5b (11), but not the closely related protein STAT5a (12, 13). STAT5b is repeatedly activated by each successive plasma GH pulse in male rats, whereas in females, the nearly continuous plasma GH profile down-regulates GHR-JAK2-STAT5b signaling (14–16). This down-regulation by continuous GH is associated with more rapid deactivation of the GHR-JAK2 signaling complex by a proteasome-dependent process (17) that may be linked to GHR internalization and/or degradation.

Factors that regulate GHR internalization and degradation are likely to contribute to down-regulation of GHR signaling (18, 19). This down-regulation is linked to GH-induced GHR internalization and degradation via the proteasome and requires an intact ubiquitination system (20). The pathway by which GHR is internalized from the cell surface is not well understood. GHR has been reported to be internalized via clathrin-coated pits (21, 22), but also may use caveolae, formed by caveolin and dependent on membrane cholesterol, as another pathway (23, 24). Inactivation of the ubiquitin-activating enzyme E1 leads to accumulation of non-ubiquitinated GHR on the cell surface (25, 26), which suggests that GHR ubiquitination and internalization are related. GHR degradation is dependent on cellular ubiquitination activity; however, the ubiquitination of GHR itself is not required for GHR to be targeted for degradation (27). Together, these findings suggest that yet unidentified proteins facilitate internalization of GHR, perhaps by acting as endocytic adaptors that are tagged by ubiquitination.

GH-induced JAK-STAT signaling is negatively regulated by proteins belonging to the SOCS family (28). The protein CIS (29), a member of the SOCS family, inhibits liver GHR signaling to STAT5b by competing with STAT5b for common GHR phosphotyrosine-binding sites and by a second mechanism that involves proteasomal action (30). The CIS gene is activated by GH via a STAT-dependent transcriptional mechanism (31), and CIS protein levels are up-regulated in association with persistent GH stimulation in the case of mice transgenic for GH-releasing hormone or bovine GH (32, 33). In primary rat hepatocytes continuously stimulated with GH, CIS mRNA is induced within 2 h and is sustained at elevated levels for at least 24 h (34). Like other members of the SOCS/CIS family, CIS contains a short N-terminal domain, a central

\* This work was supported in part by National Institutes of Health Grant DK33765 (to D. J. W.). The costs of publication of this article were defrayed in part by the payment of page charges. This article must therefore be hereby marked "advertisement" in accordance with 18 U.S.C. Section 1734 solely to indicate this fact.

<sup>1</sup> To whom correspondence should be addressed: Dept. of Biology, Boston University, 5 Cummington St., Boston, MA 02215. Fax: 617-353-7404; E-mail: djw@bu.edu.

<sup>2</sup> The abbreviations used are: GH, growth hormone; GHR, growth hormone receptor; STAT, signal transducer and activator of transcription; JAK2, Janus kinase-2; SOCS, suppressor of cytokine signaling; CIS, cytokine-inducible SH2 domain-containing protein; SH2, Src homology 2; E3, ubiquitin-protein isopeptide ligase; pAb, polyclonal antibody; mAb, monoclonal antibody; PBS, phosphate-buffered saline; PMSF, phenylmethylsulfonyl fluoride; TBS, Tris-buffered saline.

## CIS-dependent GHR Internalization

SH2 domain, and a C-terminal SOCS box (35). SOCS box-containing proteins can act as adaptor molecules that recruit activated signaling proteins to the proteasome (36). SOCS proteins associate, via their SOCS box, with elongins B and C (elongin BC complex) and cullin-2 and may thereby contribute to formation of a putative ubiquitin-protein isopeptide ligase (E3) complex that targets SOCS-associated proteins for proteasomal degradation (36). CIS can be monoubiquitinated and accumulates in this form in the presence of proteasome inhibitors (37). Moreover, the inhibitory effect of CIS on GH signaling can be blocked by proteasome inhibitors (30). These observations, together with the finding that CIS binds, via its SH2 domain, to tyrosine-phosphorylated GHR (38, 39), suggest that CIS may negatively regulate GH signaling by acting as an adaptor molecule that targets GHR to the proteasomal degradation pathway.

In this study, we investigated the cellular localization and trafficking of GHR and the role of CIS in receptor internalization following GH stimulation. Using the GH-responsive rat liver-derived cell line CWSV-1 (40) and a dominant-negative SH2 domain mutant of CIS (30, 41), we demonstrate that CIS plays an important role in the control of GHR internalization following receptor phosphorylation, leading us to propose that CIS-dependent internalization of GHR is a prerequisite for proteasome-dependent down-regulation of GH signaling.

### MATERIALS AND METHODS

**Plasmids**—The pCMV expression plasmid encoding N-terminally FLAG-tagged rabbit GHR was provided by Dr. Joelle Finidori (INSERM, Paris, France) (42). The pME18S-FLAG-CIS-R107K expression plasmid, with an SH2 domain arginine-to-lysine point mutation at residue 107 (41), and the corresponding Myc-tagged SOCS1-R105K SH2 domain mutant were from Dr. Warren Leonard (NIH, Bethesda, MD). Human CIS and SOCS6 cDNAs cloned into the expression plasmid pcDNA3 with an N-terminal Myc tag (43) were provided by Dr. Akihiko Yoshimura (Kurume University, Kurume, Japan). The pME18S-STAT5b (mouse) expression plasmid was obtained from Dr. Alice Mui (DNAX Research, Inc., Palo Alto, CA).

**Chemicals and Antibodies**—Recombinant rat GH and rabbit anti-rat GH antiserum were obtained from Dr. A. F. Parlow (National Hormone and Pituitary Program, Harbor-UCLA Medical Center, Torrance, CA). Rat GH was dissolved at a stock concentration of 0.1 mg/ml in 0.01 M NaHCO<sub>3</sub> and stored in aliquots at -80 °C. Working solutions of GH were prepared by dilution into serum-free culture medium immediately before use. Cells were stimulated with 200 ng/ml GH. Stock solutions of the proteasome inhibitors MG132 and epoxomicin (Peptides International Inc., Louisville, KY) were prepared in Me<sub>2</sub>SO. Cells were treated with 40 μM MG132 or 10 μM epoxomicin (44) diluted in serum-free medium, added 15 min prior to GH stimulation (30).

Rabbit anti-GHR C-terminal domain polyclonal antibody (pAb) 2941 (45) was provided by Drs. G. Peter Frick and H. Maurice Goodman (University of Massachusetts Medical School, Worcester, MA). Mouse anti-GHR monoclonal antibody (mAb) 263, directed against the extracellular domain of GHR (46), was purchased from Research Diagnostics Inc. (Flanders, NJ). Mouse anti-phosphotyrosine mAb 4G10 was purchased from Upstate Biotechnology Inc. (Lake Placid, NY), and mouse anti-FLAG mAb M2 was from Sigma. Mouse anti-phosphotyrosine mAb PY99 and rabbit anti-STAT5b pAb C-17 were from Santa Cruz Biotechnology, Inc. (Santa Cruz, CA). Tyrosine-phosphorylated STAT5b was detected with rabbit anti-phospho-Tyr<sup>694</sup> STAT5 mAb (Cell Signaling Technology, Inc., Beverly, MA), which recognizes phospho-Tyr<sup>699</sup> STAT5b. Alexa Fluor 488-conjugated goat anti-mouse and goat anti-rabbit IgG secondary antibodies were purchased from Molec-

ular Probes, Inc. (Eugene, OR). Horseradish peroxidase-coupled sheep anti-mouse and anti-rabbit IgG secondary antibodies were from Amersham Biosciences.

**Cell Culture and Transfection**—CWSV-1, a GH-responsive SV40-immortalized cell line derived from adult male rat hepatocytes (47), was maintained and passaged in RPCD medium with the addition of a trace element mixture ("complete RPCD medium") (40). Transfections were carried out as described previously (30) using FuGENE 6 transfection reagent (Roche Applied Science, Mannheim, Germany) at 2 μl of FuGENE 6 μg of total DNA. Twenty-four h after the addition of the FuGENE 6/DNA mixture to the cells, cells were stimulated with GH as specified in each experiment.

**Protein Extraction and Immunoprecipitation**—Cell lysates for immunoprecipitation were prepared from cells grown in 10-cm dishes. Cells were placed on ice, washed with cold phosphate-buffered saline (PBS), and incubated on ice for 30 min in 1 ml of immunoprecipitation buffer (150 mM NaCl, 1% (v/v) Triton X-100, 10 mM Tris-HCl (pH 7.6), 1 mM EDTA, 1 mM EGTA, 1 mM phenylmethylsulfonyl fluoride (PMSF), 1 mM sodium orthovanadate, and protease inhibitor mixture (Roche Applied Science)). The cells were scrapped, and cell extracts were passed through a 27-gauge needle and centrifuged. Supernatant fractions were collected, and protein concentrations were determined using a Bio-Rad protein assay kit. Endogenous GHR protein was precipitated from the cell lysates using anti-GHR pAb 2941. Cell lysates adjusted to 1 mg of total protein/ml of immunoprecipitation buffer were incubated overnight at 4 °C with pAb 2941 (1:500 dilution). Forty μl of a 50% (v/v) slurry of protein A-Sepharose beads (Amersham Biosciences) in immunoprecipitation buffer was added, and the samples were incubated for 2.5 h at 4 °C on a shaker. The immune complexes were washed three times with immunoprecipitation buffer, and precipitated proteins were released from the protein A-Sepharose beads by boiling in 2× Laemmli sample buffer (48) for 10 min, followed by Western blot analysis as described below.

**Western Blotting**—Proteins were resolved by electrophoresis on 7.5% SDS-polyacrylamide gels, transferred to nitrocellulose membranes, and blocked in blocking solution as follows. For detection of tyrosine-phosphorylated GHR, membranes were blocked for 1 h at room temperature with 3% bovine serum albumin in Tris-buffered saline (TBS)/Tween (TBST buffer; 10 mM Tris-HCl (pH 7.6), 150 mM NaCl, and 0.1% (v/v) Tween 20) and then immunoblotted overnight at 4 °C with anti-phosphotyrosine mAb 4G10 (1:1000 dilution) or PY99 (1:1000 dilution) diluted in 3% bovine serum albumin in TBST buffer. For detection of total GHR and STAT5b, membranes were blocked for 1 h at room temperature in 5% nonfat dry milk in TBST buffer and probed overnight at 4 °C with pAb 2941 (1:6000 dilution) or anti-STAT5b pAb (1:3000 dilution), respectively, diluted in 5% milk in TBST buffer. Membranes were washed (3 × 5 min) with TBST buffer and then incubated with the appropriate horseradish peroxidase-coupled secondary antibody. Proteins were visualized using ECL Plus reagent (Amersham Biosciences). Membranes were stripped in 62.5 mM Tris-HCl (pH 7.6), 2% SDS, and 50 mM β-mercaptoethanol for 20 min at 60 °C; washed (4 × 10 min) with TBST buffer; blocked in the appropriate blocking solution for 1 h at room temperature; and reprobed with primary antibody as required.

**Deglycosylation Reactions**—CWSV-1 cells grown in 10-cm dishes were lysed in 1 ml of fusion lysis buffer (1% (v/v) Triton X-100, 150 mM NaCl, 10% (v/v) glycerol, 50 mM Tris-HCl (pH 8.0), 2 mM EDTA, 1 mM PMSF, 1 mM sodium orthovanadate, and protease inhibitor mixture). Supernatants prepared from the lysates were subjected to immunoprecipitation with pAb 2941. Immune complexes were boiled for 10 min in 0.5% SDS and 1% β-mercaptoethanol supplemented with 1 mM PMSF.

Eluted proteins were collected and digested overnight at 37 °C with 1000 units of peptide *N*-glycosidase F or 1000 units of endoglycosidase H (New England Biolabs Inc., Beverly, MA) in the reaction buffers provided by the manufacturer and supplemented with 1 mM PMSF, 1 mM sodium orthovanadate, and protease inhibitor mixture. Reactions were stopped by the addition of 6× Laemmli sample buffer, followed by boiling for 10 min. Digested products were resolved on SDS-polyacrylamide gels and analyzed by Western blotting.

**Cell-surface Biotinylation**—Cell-surface biotinylation was performed on CWSV-1 cells grown in 10-cm dishes in serum-free complete RPCD medium. Cells were washed twice with ice-cold PBS (pH 8.0) and incubated for 30 min on ice with 5 ml of biotinylation reagent (0.5 mg/ml EZ-Link sulfosuccinimidyl 2-(biotinamido)-ethyl-1,3'-dithiopropionate (Pierce) freshly dissolved in PBS (pH 8.0)) with gentle shaking every 5 min. The biotinylation reagent was removed by aspiration, and the reaction was quenched by incubating cells for 15 min on ice with 10 mM Tris-HCl (pH 8.0) and 150 mM NaCl, followed by a 5-min wash with ice-cold PBS (pH 8.0). The cells were then lysed in 1 ml of fusion lysis buffer supplemented with 1 mM PMSF, 1 mM sodium orthovanadate, and protease inhibitor mixture. Biotinylated proteins were extracted from cell lysates by incubation with 40  $\mu$ l of 50% (v/v) streptavidin-Sepharose beads (Amersham Biosciences) for 3 h at 4 °C, followed by three washes of the beads with fusion lysis buffer. Proteins were recovered from the streptavidin-Sepharose beads by boiling in 2× Laemmli buffer for 10 min, followed by SDS-PAGE and Western blot analysis.

**Indirect Immunofluorescence and Confocal Microscopy**—CWSV-1 cells were seeded at 50% confluence in 2-well (2 cm<sup>2</sup>/well) chamber slides (catalog no. 154461, Nalge Nunc International, Naperville, IL) in complete RPCD medium containing 3% fetal bovine serum and allowed to adhere overnight. The medium was then replaced with fresh serum-free complete RPCD medium for at least 4 h, after which the cells were transfected for 24 h with 400 ng of FLAG-GHR alone or together with 800 ng of CIS-R107K expression plasmid. Typically, 5–10% of the cells were transfected with GHR under these conditions (compare the percent of brightly fluorescent cells indicated at time = 0 in Figs. 3A, 5A, and 6A). The percentage of brightly fluorescent cells indicated in individual experiments was determined by counting at least 15 fields, typically containing 180–300 cells. Twenty-four h after transfection, the cells were stimulated with GH as specified in each figure, washed three times with PBS, and fixed as follows. For detection of GHR, cells were fixed in 4% paraformaldehyde in PBS for 30 min at room temperature. Cells were permeabilized with 0.5% Triton X-100 for 4 min where indicated, washed with PBS, and blocked by incubation in PBS containing 10% goat serum (Sigma) for 30 min at room temperature. Antibody diluted in PBS containing 1% goat serum was then added for 1 h at room temperature. Antibody dilutions were as follows: anti-rat GH antibody, 1:1000; anti-GHR pAb 2941, 1:1000; anti-GHR mAb 263, 1:500; and anti-FLAG mAb, 1:500. The samples were washed (3 × 5 min) with PBS containing 1% goat serum and then incubated for 1 h at room temperature with Alexa Fluor 488-conjugated secondary antibody (green fluorescence) diluted 1:1000 in PBS containing 1% goat serum. Cells were washed (2 × 5 min) with 1% goat serum in PBS and then washed (1 × 5 min) with PBS alone and stained with 500  $\mu$ l of 5  $\mu$ g/ml propidium iodide (Sigma) in PBS for 10 min at room temperature to visualize the nuclei (red fluorescence). Cells were washed twice with PBS and covered with a glass coverslip using Fluoroguard anti-fade reagent (Bio-Rad). To detect STAT5b, cells were fixed in 100% methanol for 20 min at –20 °C; washed with PBS; blocked with PBS containing 3% calf serum for 1 h at room temperature; and incubated with anti-STAT5b pAb or

anti-phospho-Tyr<sup>694</sup> STAT5 mAb as described (49), except that anti-STAT5b pAb (1:500 dilution) incubations were for 1 h at room temperature and anti-phospho-Tyr<sup>694</sup> STAT5 mAb (1:500 dilution) incubations were overnight at 4 °C in a humidified environment to minimize nonspecific binding. Alexa Fluor 488-conjugated secondary antibody was used as described above.

Fluorescence was visualized using an Olympus BX-50 confocal laser scanning microscope equipped with an argon-krypton laser. For visualization of Alexa Fluor and propidium iodide staining, cells were excited at 488 or 568 nm, and emission was detected through a 510–550-nm band-pass filter (green channel) or a 610-nm long-pass filter (red channel), respectively. Image files were processed for presentation using Adobe Illustrator software.

**GH Pulse-Chase Experiments**—CWSV-1 cells grown in 2-well chamber slides were transfected for 24 h as required and treated with GH for 5 min at 37 °C to induce internalization of GHR and GH. The cells were then washed twice with ice-cold PBS (pH 7.4) to remove excess GH from the medium (“neutral wash”). Alternatively, plasma membrane-bound GH was stripped from the cell surface by a 5-min incubation with 500  $\mu$ l of acidic buffer (0.15 M NaCl and 0.05 M glycine (pH 2.5)) on ice (18), followed by washing with PBS (“acidic wash”). Cells were then fixed in 4% paraformaldehyde or returned to the tissue culture incubator, chased in GH-free culture medium at 37 °C for an additional 25 or 55 min, washed, and fixed. After a 4-min permeabilization with 0.5% Triton X-100, the cells were immunostained with anti-GH antibody, and GH was visualized using Alexa Fluor 488-conjugated secondary antibody as described above.

## RESULTS

**Dynamics of Endogenous GHR and STAT5b Tyrosine Phosphorylation**—We first established the kinetics of endogenous GHR tyrosine phosphorylation in CWSV-1 cells, which are highly responsive to GH and contain a GH-inducible STAT5b signaling pathway similar to that found in intact rat liver (40). Cells were stimulated with GH, and GHR tyrosine phosphorylation was evaluated by immunoprecipitation of GHR using anti-GHR pAb 2941, followed by Western blotting with anti-phosphotyrosine mAb 4G10. GHR tyrosine phosphorylation was detected as early as 2 min after GH stimulation. Peak tyrosine phosphorylation, seen after 30 min, was followed by dephosphorylation, which was nearly complete by 1 h (Fig. 1A, upper panel). GHR signaling to STAT5b followed a similar time course: STAT5b tyrosine phosphorylation was first detected at 5 min, was maximal at 30–40 min, and declined thereafter (Fig. 1A, lower panel, and data not shown).

Tyrosine-phosphorylated GHR protein migrated as a diffuse band of ~120 kDa (Fig. 1A, upper panel) and exhibited a lower electrophoretic mobility compared with the major non-tyrosine-phosphorylated CWSV-1 cell GHR protein, which migrated as a sharper, faster moving band of ~105 kDa (middle panel). Deglycosylation experiments demonstrated that the 120-kDa protein corresponds to mature glycosylated GHR and the 105-kDa protein to an immature precursor form. This was established by digestion of GHR immunoprecipitated from extracts of 30-min GH-stimulated CWSV-1 cells with endoglycosidase H, which cleaves the carbohydrate core of high mannose glycoproteins, or with peptide *N*-glycosidase F, which hydrolyzes nearly all types of *N*-glycan chains (50). The tyrosine-phosphorylated GHR product formed by peptide *N*-glycosidase F digestion migrated as a sharp band of ~105 kDa (Fig. 1B, upper panel), suggesting that the original 120-kDa GHR band includes ~15 kDa of carbohydrate. No increase in electrophoretic mobility was seen following endoglycosidase H digestion, suggesting that the 120-kDa band corresponds to the mature low mannose cell-

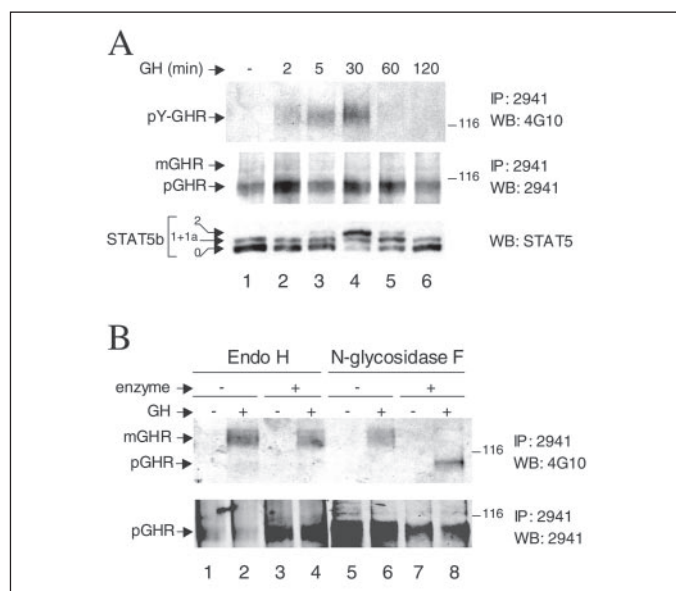


**FIGURE 1. Tyrosine phosphorylation and dephosphorylation of GHR and STAT5b in GH-stimulated CWSV-1 cells.** *A*, CWSV-1 cells were treated with 200 ng/ml GH for the times indicated. GHR protein was immunoprecipitated (IP) from total cell extracts using anti-GHR pAb 2941. Tyrosine-phosphorylated GHR (pY-GHR) and total GHR protein were visualized by Western blotting (WB) using anti-phosphotyrosine mAb 4G10 or anti-GHR pAb 2941, respectively. The positions of the mature (mGHR) and precursor (pGHR) forms of GHR are indicated. STAT5b protein was detected in total extracts by Western blotting with anti-STAT5 antibody. STAT5b band 0 represents the phosphorylated form of STAT5b; bands 1 + 1a correspond to the serine/threonine-phosphorylated (in untreated cell extracts) and tyrosine-phosphorylated (GH-treated extracts) forms of STAT5b, respectively; and band 2 represents (serine/threonine + tyrosine)-diphosphorylated STAT5b (40). *B*, immunoprecipitated GHR protein was digested with endoglycosidase H (Endo H) or peptide N-glycosidase F as indicated. The digestion products were resolved on an SDS gel and visualized on a Western blot probed with mAb 4G10 (upper panel) or in a separate experiment with pAb 2941 (lower panel). The electrophoretic mobilities of the glycosylated (mature (m)) and deglycosylated (precursor (p)) forms of GHR are indicated. Recovery of GHR was poor in the samples shown in *B* (lower panel, lanes 1 and 2).

surface GHR. No shift in the electrophoretic mobility of the non-tyrosine-phosphorylated 105-kDa GHR band was observed after digestion with either endoglycosidase H or peptide N-glycosidase F (Fig. 1*B*, lower panel), indicating that this band corresponds to an unglycosylated precursor intracellular form of the receptor.

**Visualization of Cell-surface and Intracellular GHR Proteins by Confocal Microscopy**—Next, we established a confocal immunofluorescence assay to visualize cell-surface GHR in CWSV-1 cells. We first attempted to monitor cell-surface expression of endogenous GHR, visualized by immunostaining using mAb 263, which binds to the GHR extracellular domain. Permeabilization of the cells with 0.5% Triton X-100 enabled us to detect intracellular GHR, which was randomly distributed around the nucleus, with more diffuse and faint fluorescence seen in more distant membrane areas (Fig. 2*A*, right panel). However, no cell-surface fluorescence was detected in unpermeabilized cells (Fig. 2*A*, left panel), indicating that endogenous cell-surface GHR is below the limit of detection. Thus, the major fraction of GHR protein has an intracellular localization. This conclusion is consistent with the large differences in abundance of endogenous mature cell-surface GHR (120 kDa) compared with immature intracellular GHR protein (105 kDa) seen in Fig. 1*A* (middle panel).

To visualize cell-surface GHR, CWSV-1 cells were transfected with full-length GHR containing an N-terminal FLAG tag, which enabled us to localize the receptor extracellular domain by indirect immunofluorescence using anti-FLAG mAb. Fluorescently labeled cells were scanned from top to bottom in 1- $\mu$ m steps (optical z sections) to evaluate the distribution of GHR on the cell surface and inside the cell.

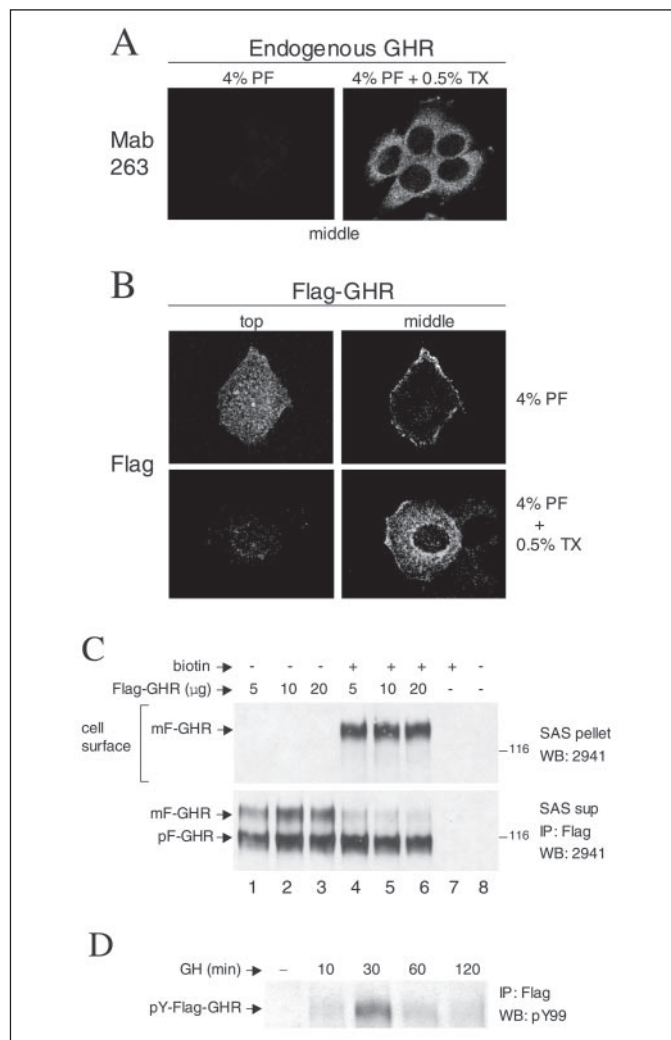


**FIGURE 2. Cell-surface and intracellular GHR proteins in CWSV-1 cells.** *A* and *B*, CWSV-1 cells, untransfected (*A*) or transfected (*B*) with N-terminally FLAG-tagged GHR (400 ng), were fixed in 4% paraformaldehyde (PF) for 30 min, permeabilized or not permeabilized with 0.5% Triton X-100 (TX) as indicated, and immunostained with anti-FLAG mAb or anti-GHR mAb 263 (raised against the extracellular domain of GHR) as described under "Materials and Methods." Shown are optical z sections through the top or middle of the cells as indicated. *C*, CWSV-1 cells were transfected with the indicated amounts of FLAG-GHR, labeled with EZ-Link sulfo succinimidyl 2-(biotinamido)-ethyl-1,3'-dithiopropionate (see "Materials and Methods"), and lysed. Biotinylated cell-surface proteins were isolated from the cell lysates using streptavidin-Sepharose (SAS) (upper panel). Material remaining in the supernatant (SAS sup) was immunoprecipitated (IP) with anti-FLAG mAb (lower panel). Samples were resolved on an SDS gel and analyzed by Western blotting (WB) with pAb 2941 as indicated. The precursor form of FLAG-GHR (pF-GHR) was found exclusively in the intracellular fraction (anti-FLAG immunoprecipitate of the streptavidin-Sepharose supernatant). The mature form (mF-GHR) was found primarily on the cell surface (i.e. in the streptavidin-Sepharose pellet fraction); the small amount of the mature form present in the streptavidin-Sepharose supernatant fraction (lower panel, lanes 4–6) may reflect newly synthesized mature GHR that did not yet reach the cell surface or cell-surface GHR that was not efficiently biotinylated. The mature GHR protein band (lower panel, lanes 1–3) represents total (i.e. cell-surface + intracellular) mature GHR. *D*, CWSV-1 cells were transfected with FLAG-GHR and treated with GH for the times indicated. FLAG-GHR was immunoprecipitated from cell lysates with anti-FLAG mAb and analyzed by Western blotting with anti-phosphotyrosine mAb PY99. pY-Flag-GHR, tyrosine-phosphorylated, FLAG-tagged GHR.

Representative z sections are presented in Fig. 2*B*. In cells fixed in 4% paraformaldehyde without detergent permeabilization, GHR was detected in small, randomly distributed granules on the cell surface (Fig. 2*B*, upper left panel). Little or no immunostaining was detected in the cytoplasm when optical z sectioning was carried out through the middle of the cell (Fig. 2*B*, upper right panel). In contrast, in detergent-permeabilized cells (Fig. 2*B*, lower panels), diffuse fluorescent labeling over the

entire cytoplasm was seen, with some accumulation in the perinuclear area.

To further analyze the intracellular distribution of GHR, CWSV-1 cells transfected with FLAG-GHR were biotinylated using a membrane-impermeable reagent. Biotinylated cell-surface GHR was isolated using streptavidin-Sepharose, whereas non-biotin-labeled (*i.e.* intracellular) GHR was recovered from the supernatant remaining after streptavidin-Sepharose precipitation by immunoprecipitation using anti-FLAG mAb. Cell-surface and intracellular FLAG-GHR proteins were both visualized by immunoblotting using anti-GHR antibody (Fig. 2C). In the streptavidin-Sepharose precipitates, FLAG-GHR appeared as a single ~125-kDa band, corresponding to the mature cell-surface receptor (Fig. 2C, upper panel, lanes 4–6) (51), with the peak of tyrosine phosphorylation at 30 min of GH treatment (Fig. 2D). In the anti-FLAG immunoprecipitates, FLAG-GHR was visualized as two bands of ~110 and ~125 kDa, corresponding to the precursor and mature intracellular forms of FLAG-GHR, respectively (Fig. 2C, lower panel, lanes 4–6). No biotin-labeled endogenous cell-surface GHR was detected in untransfected cells (Fig. 2C, upper panel, lane 7), supporting our conclusion that there is a very low level of endogenous GHR at the cell surface (*cf.* Fig. 2A).

Given the low level of endogenous cell-surface GHR expression, all of our subsequent experiments were carried out in cells transfected with FLAG-tagged GHR. This enabled us to monitor cell-surface GHR and its internalization in the form of a GH·GHR complex using antibody to the GHR extracellular domain (mAb 263) or its N-terminal FLAG tag or antibody to the bound GH ligand. In control experiments, no difference was observed in the time course of GH-induced STAT5b activation and nuclear signaling in GHR-transfected cells compared with untransfected cells (data not shown).

**GHR Is Rapidly Internalized in GH-stimulated CWSV-1 Cells**—GHR internalization was assayed in cells treated with GH for 5, 30, or 60 min and was monitored in unpermeabilized cells stained with anti-GHR mAb 263 (Fig. 3A) or in unpermeabilized and permeabilized cells stained with anti-GH antibody (Fig. 3B). Immunofluorescent images were collected based on scans through the top or the middle of each cell using fixed laser intensity settings. GHR internalization was rapid, as indicated by the substantial decrease in cell-surface fluorescence associated with GHR (Fig. 3A, lanes 1 and 2) and GH (Fig. 3B, lane 1) beginning 5 min after GH addition. Similar results were obtained using a third antibody (anti-FLAG mAb) to monitor GHR internalization (see Fig. 5A, lane 1), indicating that the decrease in cell-surface GHR immunofluorescence reflects GHR internalization rather than loss of a GHR conformation-dependent antigenic determinant upon GH binding. This conclusion is strengthened by our finding that the time course for the loss of cell-surface GH and GHR immunoreactivity paralleled the appearance in the cytosol of bright fluorescent granules containing internalized GH (Fig. 3B, lane 2). GHR was no longer detectable at the cell surface after 30 and 60 min of GH stimulation, indicating complete internalization of the receptor. Given the rapid internalization of GHR following GH stimulation (Fig. 3) and our previous finding that GHR activation and signaling to STAT5b continue for 40–60 min in this same cell model (Ref. 52; also see Fig. 2D), we conclude that GHR signaling to STAT5b and the subsequent deactivation of the GHR·JAK2 signaling complex both proceed from an intracellular compartment.

**Effect of the CIS-R107K SH2 Domain Mutant on GHR Internalization**—GH-stimulated STAT5b activation is partially inhibited in cells in which CIS is expressed constitutively, reflecting an apparent competition between CIS and STAT5b for common phosphotyrosine-binding sites on GHR (30, 38). CIS-R107K, a dominant-negative CIS mutant with an

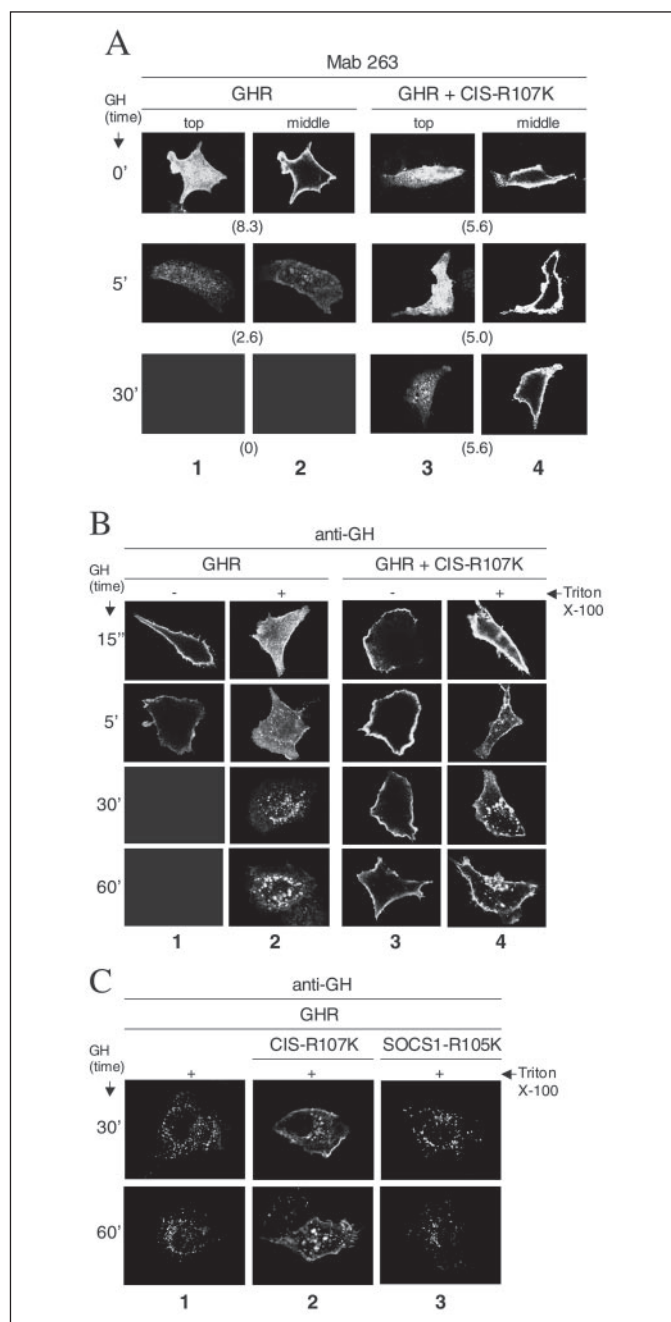


**FIGURE 3. Rapid internalization of GHR in continuously GH-treated CWSV-1 cells and inhibitory effect of CIS-R107K.** CWSV-1 cells were transfected with FLAG-GHR (400 ng) alone or in combination with 800 ng of CIS-R107K or SOCS1-R105K. Cells were treated with GH (200 ng/ml) for 5, 30, or 60 min. *A*, GH-treated cells were fixed in 4% paraformaldehyde without detergent permeabilization and immunostained with anti-GHR mAb 263. Optical z sections were taken through the top or middle of the cells as indicated. *B*, GH-treated cells were fixed in 4% paraformaldehyde with (+) or without (–) Triton X-100 permeabilization as indicated and immunostained using anti-GH antibody. Optical z sections were taken through the middle of the cells. *C*, cells were stimulated with GH for 5 min and washed with neutral wash buffer (pH 7.4) as described under “Materials and Methods,” and GHR trafficking was then monitored in GH-free medium for an additional 25 or 55 min (30- and 60-min samples, respectively). Cells were fixed in 4% paraformaldehyde, permeabilized with Triton X-100, and immunostained with anti-GH antibody. The cell images shown are representative of a total of 15 fields collected for each treatment; the number of fluorescent cells expressed as a percentage of the total number of cells examined for each treatment is indicated in parentheses in *A*. The results showing CIS-R107K inhibition of GH and GHR internalization were reproduced in at least three independent series of experiments.

inactivating mutation in the SH2 domain, reverses this inhibition, despite its inability to bind tyrosine-phosphorylated GHR (30). To further elucidate the mechanism for the dominant-negative action of CIS-

## CIS-dependent GHR Internalization

R107K, we investigated the impact of CIS-R107K on GH-induced GHR internalization. Cells were transfected with GHR alone or with CIS-R107K, and GH-GHR complex trafficking was monitored using anti-GHR mAb 263. CIS-R107K had no effect on the fluorescence intensity of cell-surface GHR either prior to or immediately (within 15 s) after GH treatment (Fig. 3A, upper panels, lanes 3 and 4 versus lanes 1 and 2) (data not shown). However, CIS-R107K exerted a striking inhibition of GH-stimulated GHR internalization monitored after 5 and 30 min of GH treatment, as illustrated in Fig. 3A and as supported by quantitation of the percentage of cells (indicated in parentheses) with detectable cell-surface GHR fluorescence (lanes 3 and 4 versus lanes 1 and 2). The same result was obtained when the effect of CIS-R107K on GHR internalization was monitored using anti-FLAG mAb (see Fig. 5A, lane 2). No significant fluorescent signal was detected in untransfected cells or in cells transfected with CIS-R107K alone (data not shown), verifying the GHR dependence of these signals. The inhibitory effect of CIS-R107K was also apparent when GH internalization was monitored using anti-GH antibody. Thus, plasma membrane-associated GH fluorescence persisted for at least 60 min in cells that expressed CIS-R107K (Fig. 3B, lane 3 versus lane 1). Analysis of detergent-permeabilized cells further revealed, however, that the inhibitory effect of CIS-R107K on GH internalization was only partial, *i.e.* complete internalization of GH within 30 min in cells devoid of CIS-R107K (Fig. 3B, lane 2) versus partial internalization of GH at 30 and 60 min in cells containing CIS-R107K (lane 4). Finally, the specificity of the GHR internalization inhibitory effect of CIS-R107K was established in experiments using two corresponding SH2 domain mutants of SOCS1 (SOCS1-R105K and SOCS1-R105E), which are devoid of dominant-negative activity (30) and were without effect on GH-induced GHR internalization (Fig. 3C, lane 3 versus lane 1) (data not shown).

We considered the possibility that the apparent persistence of cell-surface GH fluorescence in the cells expressing CIS-R107K might reflect 1) enhanced synthesis and maturation of GHR protein at the cell surface or 2) enhanced recycling of GH-GHR complexes back to the cell surface in the presence of CIS-R107K rather than inhibition of GH-GHR complex internalization *per se*. To test the first possibility, CWSV-1 cells were treated with GH applied as a 5-min pulse, sufficient to induce internalization of GHR, after which the cells were washed, and GH-GHR complex internalization was monitored in GH-free medium. GH-associated plasma membrane fluorescence persisted at 30 and 60 min in the cells expressing CIS-R107K, despite the absence of GH in the culture medium (Fig. 4, lanes 4 and 5 versus lanes 1 and 2). Thus, the persistence of the cell-surface GH signal is not the result of GH binding to newly synthesized receptor protein that appears on the cell surface. Moreover, when the 5-min GH-treated cells were washed with acidic buffer to remove cell surface-bound GH (compare the 5-min samples in Fig. 4, upper panels, lane 3 versus lane 2) (20), no cell-surface GH was detected in the CIS-R107K cells at 30 or 60 min (lane 6). Thus, CIS-R107K does not stimulate recycling of internalized GH-GHR complexes back to the cell surface. Taken together, these findings establish that CIS-R107K inhibits internalization of GH-GHR complexes from the cell surface. Given the specificity of CIS-R107K for blocking the GHR signaling inhibitory actions of CIS, but not those of other SOCS/CIS family members (30), and given the inactivity of SOCS1-R105K shown above (Fig. 3C), these findings implicate CIS as playing a specific role in GH-stimulated GHR internalization.

As an additional control, we verified the specificity of the CIS-R107K inhibitory effect as judged by the ability of exogenous wild-type CIS to compete with CIS-R107K in blocking GHR internalization. In cells transfected with GHR and CIS-R107K either alone or together with CIS,

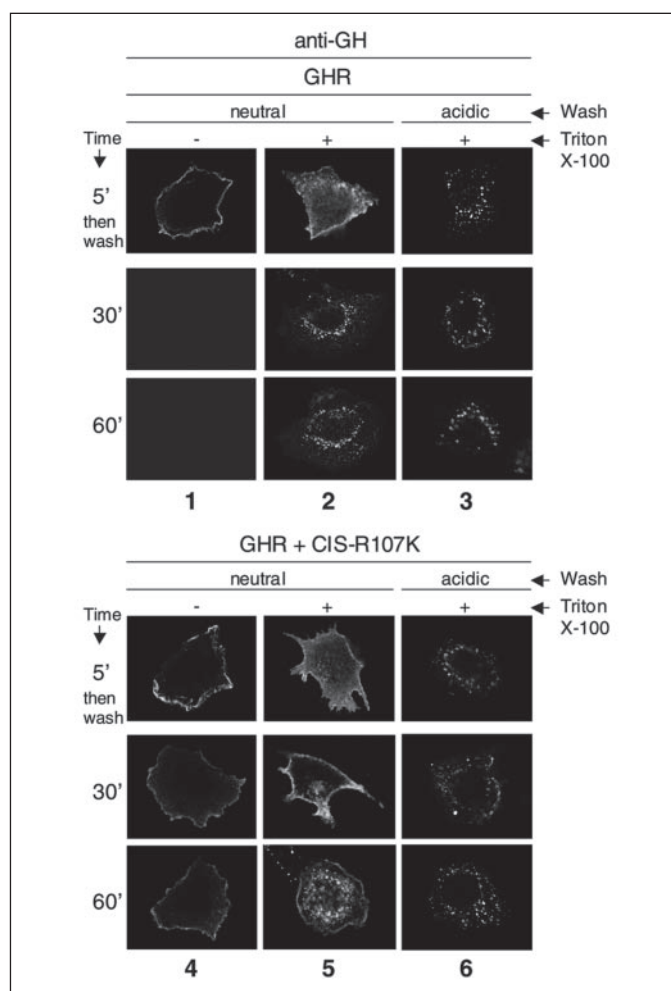


**FIGURE 4. CIS-R107K blocks GH pulse-induced GHR internalization.** CWSV-1 cells were transfected with 400 ng of FLAG-GHR alone or in combination with CIS-R107K (800 ng) as indicated. Cells were stimulated with GH (200 ng/ml) for 5 min and then washed with neutral (pH 7.4) or acidic (pH 2.5) wash buffer as described under "Materials and Methods." GHR trafficking was monitored in GH-free medium for an additional 25 or 55 min (30- and 60-min samples, respectively). Cells were fixed in 4% paraformaldehyde with (+) or without (–) Triton X-100 permeabilization as indicated and immunostained with anti-GH antibody. The cell images shown are optical z sections through the middle of the cells and are representative of a total of 15 fields collected for each treatment. The results were reproduced in at least three independent experiments.

wild-type CIS blocked the ability of CIS-R107K to inhibit GH-stimulated GHR internalization (Fig. 5, A and B, lanes 3 versus lanes 2). Wild-type CIS alone may accelerate GHR internalization (compare 1% fluorescent cells 5 min after GH addition in the case of CIS-transfected cells versus 3.2% fluorescent cells in the absence of CIS) (Fig. 5A, lane 4 versus lane 1). The inhibitory effect of exogenous CIS on CIS-R107K-inhibited GHR internalization was not due to nonspecific competition for factors required for CIS-R107K expression, as demonstrated by the inability of another SOCS/CIS family member, SOCS6 (cloned into the same plasmid backbone as wild-type CIS), to reverse the effects of CIS-R107K. Thus, SOCS6 neither blocked the inhibitory effect of CIS-R107K on GH internalization (Fig. 5B, lane 4 versus lane 2) nor blocked internalization of GH itself (lane 5 versus lane 1), confirming the specificity of CIS-R107K for inhibition of the action of CIS compared with SOCS6.

**Effect of Proteasome Inhibitors MG132 and Epoxomicin on GHR Internalization**—CIS down-regulates GHR signaling to STAT5b by a proteasome-dependent mechanism (30). In view of the role of CIS in GHR internalization demonstrated above, we investigated whether this proteasome-dependent process involves GHR internalization. CWSV-1

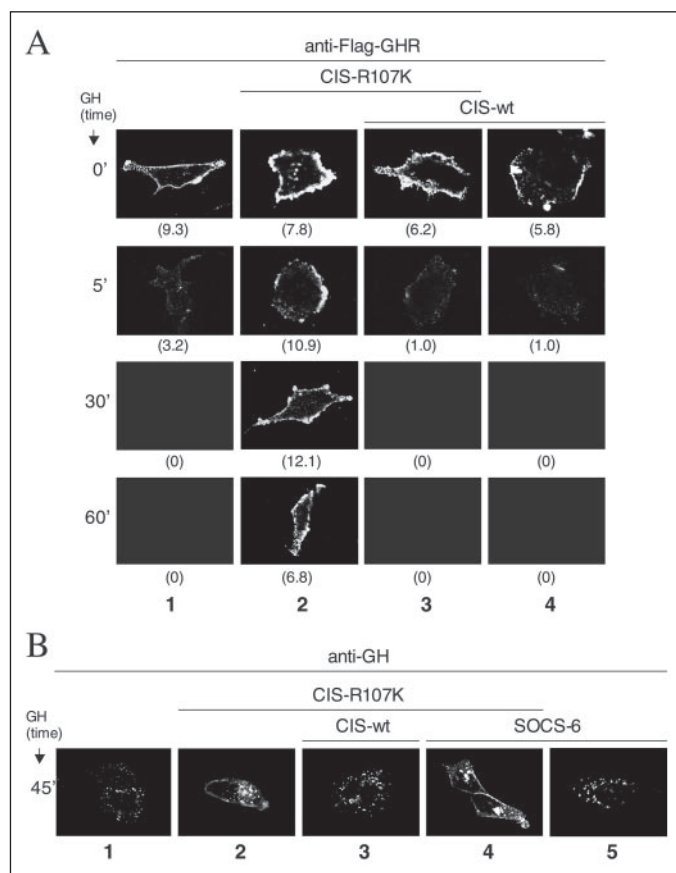


**FIGURE 5. Wild-type CIS reverses the inhibitory effect of CIS-R107K on GH-induced GHR internalization.** CWSV-1 cells were transfected with 400 ng of FLAG-GHR alone or in combination with CIS-R107K (800 ng), wild-type CIS (*CIS-wt*; 800 ng), and/or SOCS6 (800 ng) as indicated. Cells were treated with GH (200 ng/ml), fixed in 4% paraformaldehyde without detergent permeabilization, and immunostained with anti-FLAG mAb (A) or permeabilized with Triton X-100 and immunostained with anti-GH antibody (B). In control experiments (not shown), no immunofluorescence was observed in cells transfected with FLAG-tagged CIS-R107K either alone or in combination with non-FLAG-tagged GHR. Thus, the fluorescence seen in this figure is that of FLAG-GHR. Shown are optical z sections through the middle of the cells. The cell images shown in A are representative of a total of 15 fields collected for each treatment; the percentage of fluorescent cells in each sample is indicated in *parentheses*. The results were reproduced in at least three independent experiments.

cells were transfected with GHR, treated with the proteasome inhibitor MG132 for 15 min, and then stimulated with GH in the continued presence of MG132. GHR internalization was monitored by immunostaining unpermeabilized cells using anti-FLAG-GHR antibody (Fig. 6A). MG132 inhibited GH-induced internalization of GHR, similar to that seen in cells expressing CIS-R107K. Thus, after 30 and 60 min of GH treatment, the fluorescence intensity of cell-surface GHR was still detectable in cells pretreated with MG132 compared with non-MG132-treated controls (Fig. 6A, lane 2 versus lane 1). MG132 alone had no major effect on the expression of cell-surface GHR during the time frame of these experiments (Fig. 6A, lane 3). In a GH pulse-chase study, we found that the inhibitory effect of MG132 on GH internalization was partial, as determined by anti-GH immunostaining of detergent-permeabilized cells (Fig. 6B, lane 2 versus lane 1). As was the case for CIS-R107K (Fig. 4), the addition of an acidic wash to remove plasma membrane-bound GH confirmed that the persistence of GH at the cell surface in MG132-treated cells (Fig. 6B, lane 2) was not due to recycling of internalized GH-GHR complexes back to the cell surface at 30 and 60 min (lane 3). A similar partial inhibitory effect on GH internalization was observed in pulse-chase experiments using epoxomicin, which is a more specific proteasome inhibitor (Fig. 6B, lane 4).

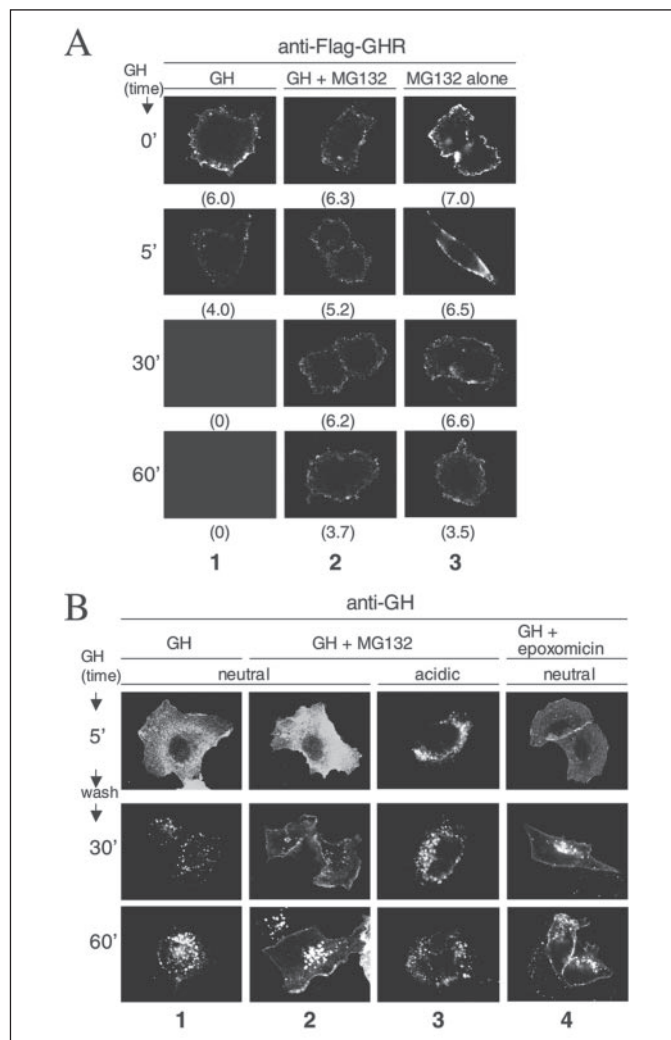


**FIGURE 6. Proteasome inhibitors MG132 and epoxomicin partially block GH-induced internalization of GH and GHR.** CWSV-1 cells were transfected for 24 h with 400 ng of FLAG-GHR and then stimulated with GH (200 ng/ml) for times up to 60 min. MG132 (40  $\mu$ M) or epoxomicin (10  $\mu$ M) was added 15 min prior to GH stimulation. A, cells were continuously stimulated with GH, fixed in 4% paraformaldehyde without detergent permeabilization, and immunostained with anti-FLAG mAb. B, cells were stimulated with a 5-min GH pulse and washed with neutral or acidic wash buffer (see "Materials and Methods"). GHR trafficking was monitored in GH-free medium for 30 or 60 min. Cells were then fixed in 4% paraformaldehyde, permeabilized with Triton X-100, and immunostained with anti-GH antibody. Optical z sections were taken through the middle of the cells. The cell images shown are representative of a total of 15 fields collected for each treatment; the percentage of fluorescent cells in each sample is indicated in *parentheses* in A. The results were reproduced in at least three independent experiments.

MG132 prolongs STAT5b DNA-binding activity in GH-treated CWSV-1 cells (52). MG132 also prolonged the tyrosine-phosphorylated nuclear STAT5b signal for at least 120 min, as demonstrated by confocal immunofluorescence analysis using anti-phospho-Tyr<sup>694</sup> STAT5 mAb (compare the 120-min samples in Fig. 7, lower panels, lane 5 versus lane 2 and lane 4 versus 1). MG132 did not alter the time course of STAT5b tyrosine phosphorylation and nuclear translocation (compare the 5- and 30-min samples in Fig. 7, middle panels). However, MG132 did inhibit the deactivation of GHR signaling to STAT5b, such that STAT5b remained tyrosine-phosphorylated and in the nucleus for at least 120 min after the initial GH treatment.

## DISCUSSION

CIS and other SOCS family proteins are negative feedback regulators of cytokine receptor signaling, including GHR signaling to STAT5b (32,

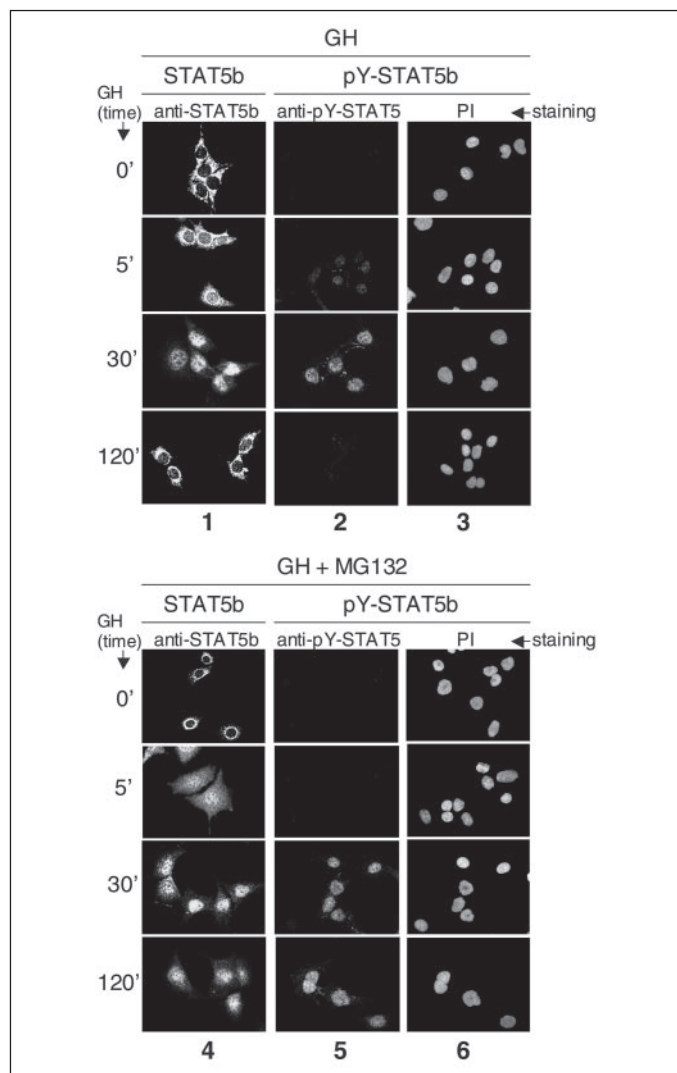


**FIGURE 7. MG132 treatment prolongs GH-induced STAT5b nuclear signaling.** CWSV-1 cells were stimulated with GH (200 ng/ml) for 5, 30, or 120 min, and the subcellular localization of STAT5b was monitored by indirect immunofluorescence using anti-STAT5b pAb or anti-phospho-Tyr<sup>694</sup> STAT5 mAb (*anti-pY-STAT5*). Nuclei were stained with propidium iodide (PI). Shown are confocal microscope images of representative fields of cells. GH induced nuclear translocation of tyrosine-phosphorylated STAT5b (*pY-STAT5b*) by 30 min, with subsequent dephosphorylation and return of STAT5b protein to the cytoplasm by 120 min. MG132 blocked down-regulation of the nuclear STAT5b signal.

38, 53, 54). In particular, CIS has been proposed to play an important role in down-regulation of the GHR-JAK2-STAT5b signaling pathway in cells continuously exposed to GH (30) and exerts its inhibitory effect by binding to phosphotyrosine residues in the cytoplasmic domain of GHR (38). CIS inhibits GHR signaling to STAT5b by two distinct mechanisms: 1) by competition with STAT5b for common tyrosine-binding sites on the cytoplasmic tail of GHR and 2) by a proteasome-dependent mechanism that involves degradation of CIS, perhaps in association with the GHR-JAK2 signaling complex (30). In this study, we investigated the role of CIS and the proteasome in GH-stimulated internalization of GHR. Using the rat liver cell line CWSV-1 as a model, we have demonstrated the following. 1) GHR signaling to STAT5b is initiated at the cell surface, but continues from an intracellular compartment following GHR internalization; and 2) CIS plays an important role in GHR internalization, which is an essential prerequisite for termination of receptor signaling.

A confocal immunofluorescence assay was established to investigate

the internalization of GHR in GH-treated CWSV-1 liver cells, which contain an endogenous GHR-STAT5b signaling pathway. We found that the major fraction of GHR expressed endogenously in these cells has an intracellular localization and that endogenous cell-surface GHR is below the limit of immunofluorescence detection. Accordingly, we carried out our subsequent experiments using CWSV-1 cells transfected with FLAG-tagged GHR, which allowed us to monitor the trafficking of the GH-GHR complex from the cell surface. The activation of GHR signaling by GH was accompanied by tyrosine phosphorylation of GHR (peak phosphorylation at 30 min) and by internalization of a GH-GHR complex, as revealed by anti-GHR and anti-GH immunofluorescence analysis. The tyrosine-phosphorylated form of GHR was characterized as a mature form of the receptor (39, 55, 56) of ~125 kDa. GH pulse-chase experiments established that the ligand-activated receptor was internalized after 5 min of GH treatment and was not recycled back to the cell surface in significant amounts. Despite the rapid down-regulation of cell-surface GHR, signaling from the receptor to STAT5b continued for at least an additional 30–40 min, indicating that a major fraction of GHR signaling to STAT5b and the subsequent deactivation of the GHR-JAK2 signaling complex proceed from an intracellular compartment.

CWSV-1 cells show a relatively high level of GH-induced endogenous CIS mRNA (38), which appears within 60 min of GH stimulation, *i.e.* in a time course that correlates with the time course of termination of GHR signaling to STAT5b. To investigate the role of CIS in GHR internalization, we used a dominant-negative SH2 domain mutant of CIS, CIS-R107K (41), which, despite its inability to bind to tyrosine-phosphorylated GHR, blocks the inhibitory effect of CIS on GHR signaling to STAT5b, but not the inhibitory effects of other SOCS proteins (30). In this study, CIS-R107K blocked internalization of GHR from the cell surface, and this inhibitory effect was reversed when exogenous wild-type CIS (but not SOCS6) was introduced together with CIS-R107K. As a consequence of the inhibition by CIS-R107K, GHR remained on the cell surface for a prolonged period of time, at least 1 h in this study. Correspondingly, CIS-R107K exerts a dominant-negative effect on the continuous GH-induced desensitization of endogenous GHR signaling to STAT5b that normally occurs within ~1 h of GH stimulation in the same liver cell line (30). Although retention of GHR on the cell surface is not required for ongoing GHR signaling, as noted above, it nevertheless has the effect of prolonging GHR signaling to STAT5b. This strongly suggests that GHR internalization is an obligatory prerequisite step for receptor down-regulation and signal termination. Thus, by blocking GHR internalization, CIS-R107K allows GHR to escape (or at least forestall) the intracellular events that lead to receptor deactivation, enabling the receptor to continue signaling to STAT5b and presumably other downstream targets.

The mechanism for the dominant-negative action of CIS-R107K is unknown. CIS-R107K contains an SH2 domain-inactivating point mutation and is unable to compete with CIS for its phosphotyrosine binding sites on GHR (30). Presumably, CIS-R107K competes with endogenous CIS for factor(s) that act downstream of GHR-CIS binding and that are required for GHR internalization. These factors may include elongins B and C, which interact with SOCS/CIS proteins via their C-terminal SOCS box (57–59) and facilitate recruitment of cullin-2 and formation of an E3 complex (36, 57). SOCS1 has been shown to promote SOCS box-dependent ubiquitination and proteasomal degradation of JAK2 and other SOCS1-interacting proteins (60). A similar SOCS box-mediated mechanism was proposed for termination of insulin receptor signaling by SOCS1 and SOCS3, which have been suggested to target insulin receptor substrate-1 and -2 for SOCS box-dependent,

ubiquitin-mediated degradation (61), and this type of mechanism may be used by CIS as well. CIS can be monoubiquitinated (37); is subject to proteasomal degradation (30); and has a modular structure similar to SOCS1 and SOCS3, including a conserved SH2 domain and SOCS box. CIS may therefore serve as an adaptor protein that recruits an E3 complex through its SOCS box while binding to tyrosine-phosphorylated GHR through its SH2 domain. This would lead, in turn, to ubiquitination of GHR at the cell surface, introducing a sorting signal for receptor internalization, intracellular trafficking, and degradation (62). Our finding that the GHR internalization inhibitory action of CIS-R107K was not observed with the corresponding SH2 domain mutant of SOCS1 demonstrates specificity with respect to CIS and presumably the SOCS box of CIS in this regard. Given the finding that GHR ubiquitination *per se* is not required for proteasome-dependent degradation of GHR (27), CIS bound to GHR in association with an E3 complex may be sufficient to tag the receptor for internalization and degradation. According to this model, competition between CIS-R107K and endogenous CIS for binding to the E3 complex would lead to the observed inhibition of GHR internalization.

The inhibitory effect of CIS-R107K and that of the proteasome inhibitors MG132 and epoxomicin on GH-GHR internalization were incomplete, as revealed by the appearance of cytosolic granular structures containing GH (and possibly also GHR) within the cytosol. This finding suggests that GHR internalizes by two distinct pathways, only one of which is dependent on CIS and subject to inhibition by CIS-R107K. Conceivably, these two pathways may correspond to the clathrin-coated pit pathway (21, 22) and the caveolin pathway for GHR internalization (23, 24) described previously. A precedent for the possibility that GHR may be internalized by multiple pathways is provided by studies of the epidermal growth factor receptor, the internalization and degradation of which is regulated by the E3 ligase c-Cbl and independently by SOCS4 and SOCS5 (63, 64). c-Cbl down-regulates epidermal growth factor signaling by catalyzing receptor ubiquitination, which targets the receptor into clathrin-coated pits and leads to receptor endocytosis and internalization (65). Little is known about the effect of c-Cbl on cytokine receptors such as GHR. c-Cbl is tyrosine-phosphorylated in response to GH (66), and repression of c-Cbl results in enhanced colony-stimulating factor receptor JAK-STAT signaling (67). c-Cbl is also a negative regulator of STAT1 and STAT5 protein synthesis (68), erythropoietin-induced STAT5 activation (69), and GH-stimulated STAT5-mediated transcription (70). Further study is required to determine whether c-Cbl or other E3 ligases contribute to either the CIS-dependent or CIS-independent component of GHR internalization described in this study.

Proteasome inhibitors may prolong GHR signaling to STAT5b by one or more mechanisms: 1) by inhibition of a tyrosine phosphatase that contributes to GHR inactivation (52), 2) by inhibition of GHR internalization (Fig. 6) (20), and 3) by protection of GHR from proteasomal degradation (71). The partial block of GH-induced GHR internalization described here for cells treated with the proteasome inhibitors MG132 and epoxomicin is consistent with previous studies by Strous and co-workers (20, 72) showing that GHR endocytosis is highly dependent on an active ubiquitin-proteasome system: the half-life of the mature receptor (~75 min) is prolonged by 2.5-fold (to ~180 min) when ubiquitin-proteasome-dependent endocytosis is impaired. Proteasome inhibitor-dependent blocking of GHR internalization may involve ubiquitinated CIS (Fig. 8), as suggested by a study of the erythropoietin receptor (37). Our finding that the partial inhibitory action of CIS-R107K on GH internalization is no more complete when cells are additionally treated with MG132 (data not shown) lends support to this proposal and suggests that CIS-R107K and MG132 both act along the

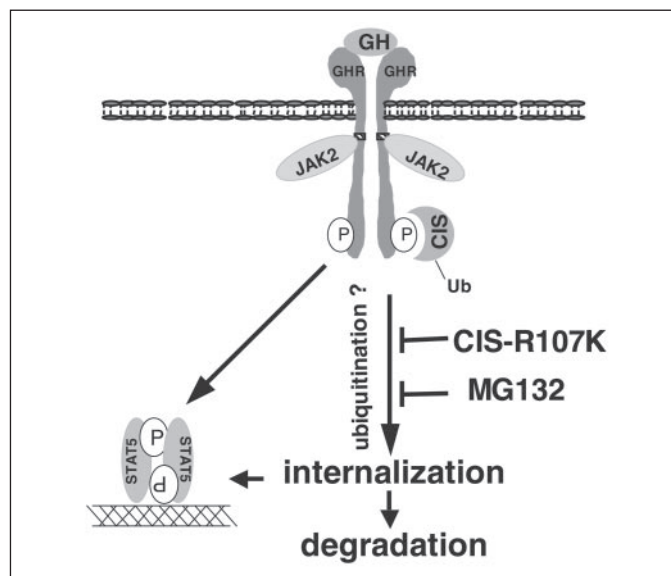


**FIGURE 8. Model for cooperation between CIS and the proteasome in the regulation of GHR internalization from the plasma membrane.** Internalization of GHR is proposed to proceed by two pathways (see "Discussion"), one of which (diagrammed here) is dependent on CIS. CIS is proposed to target GH-activated GHR to the endocytic machinery, followed by degradation of the GH-GHR-JAK2 complex. The dominant-negative SH2 domain mutant of CIS (CIS-R107K) blocks GHR internalization. This dominant-negative effect may involve competition by CIS-R107K for ubiquitination (Ub) of CIS or a CIS-associated E3 ligase (not shown), which targets GHR for endocytosis and degradation. CIS-R107K and MG132 partially inhibit GHR internalization and hence the rate of GHR signal termination. Intracellular signaling from GHR to STAT5b is therefore prolonged in the presence of CIS-R107K or MG132. The internalized GH-GHR-JAK2 signaling complex continues to activate STAT5b by tyrosine phosphorylation for ~40 min until it is inactivated.

same pathway to block internalization. The precise mechanism by which the proteasome may regulate CIS-dependent GHR internalization and degradation is not known. Proteasomal action precedes GHR endocytosis (20) and may include cleavage of a putative internalization inhibitory factor bound to GHR, thereby enabling GHR endocytosis and internalization to proceed. GHR internalization may be dependent on a ubiquitin-dependent endocytosis motif (21), which can provide a docking site for adaptor proteins such as c-Cbl, Eps15, adaptor protein-2, and clathrin, which contribute to the internalization of other receptor proteins regulated by a ubiquitin-dependent endocytosis motif (65).

In conclusion, the specific inhibitory effects of CIS-R107K on GHR internalization reported here implicate CIS in the control of GHR internalization and support the proposal that CIS acts as an adaptor protein or cofactor that targets GHR for internalization and degradation (Fig. 8). Given the inability of CIS-R107K to bind directly to and compete with CIS for GHR binding, we favor the proposal that CIS-R107K competes with CIS for ubiquitination or for binding to an adaptor protein or other downstream interacting factors, which serve as prerequisites for GHR internalization and signal termination.

**Acknowledgments**—We thank Drs. Marc Edery, Joelle Finidori, Alice Mui, Akihiko Yoshimura, and Warren Leonard for plasmid DNAs and Drs. G. Peter Frick and H. Maurice Goodman for the gift of anti-GHR pAb 2941.

## REFERENCES

- Piwiń-Pilipuk, G., Huo, J. S., and Schwartz, J. (2002) *J. Pediatr. Endocrinol. Metab.* **15**, 771–786
- Zhu, T., Goh, E. L., Graichen, R., Ling, L., and Lobie, P. E. (2001) *Cell. Signal.* **13**, 599–616
- Wan, Y., McDevitt, A., Shen, B., Smythe, M. L., and Waters, M. J. (2004) *J. Biol. Chem.* **279**, 44775–44784

4. Frank, S. J. (2002) *Endocrinology* **143**, 2–10
5. Ram, P. A., Park, S. H., Choi, H. K., and Waxman, D. J. (1996) *J. Biol. Chem.* **271**, 5929–5940
6. Smit, L. S., Meyer, D. J., Billestrup, N., Norstedt, G., Schwartz, J., and Carter-Su, C. (1996) *Mol. Endocrinol.* **10**, 519–533
7. Herrington, J., Smit, L. S., Schwartz, J., and Carter-Su, C. (2000) *Oncogene* **19**, 2585–2597
8. Darnell, J. E., Jr. (1997) *Science* **277**, 1630–1635
9. Jansson, J.-O., Ekberg, S., and Isaksson, O. (1985) *Endocr. Rev.* **6**, 128–150
10. Ahluwalia, A., Clodfelter, K. H., and Waxman, D. J. (2004) *Mol. Endocrinol.* **18**, 747–760
11. Udy, G. B., Towers, R. P., Snell, R. G., Wilkins, R. J., Park, S. H., Ram, P. A., Waxman, D. J., and Davey, H. W. (1997) *Proc. Natl. Acad. Sci. U. S. A.* **94**, 7239–7244
12. Teglund, S., McKay, C., Schuetz, E., van Deursen, J. M., Stravopodis, D., Wang, D., Brown, M., Bodner, S., Grosveld, G., and Ihle, J. N. (1998) *Cell* **93**, 841–850
13. Park, S. H., Liu, X., Hennighausen, L., Davey, H. W., and Waxman, D. J. (1999) *J. Biol. Chem.* **274**, 7421–7430
14. Waxman, D. J., Ram, P. A., Park, S. H., and Choi, H. K. (1995) *J. Biol. Chem.* **270**, 13262–13270
15. Choi, H. K., and Waxman, D. J. (2000) *Endocrinology* **141**, 3245–3255
16. Tannenbaum, G. S., Choi, H. K., Gurd, W., and Waxman, D. J. (2001) *Endocrinology* **142**, 4599–4606
17. Gebert, C. A., Park, S. H., and Waxman, D. J. (1999) *Mol. Endocrinol.* **13**, 213–227
18. Strous, G. J., and van Kerkhof, P. (2002) *Mol. Cell. Endocrinol.* **197**, 143–151
19. Kuhn, E. R., Vleurick, L., Ederly, M., Decuyper, E., and Darras, V. M. (2002) *Comp. Biochem. Physiol. B Comp. Biochem. Mol. Biol.* **132**, 299–308
20. van Kerkhof, P., Govers, R., Alves dos Santos, C. M., and Strous, G. J. (2000) *J. Biol. Chem.* **275**, 1575–1580
21. Sachse, M., van Kerkhof, P., Strous, G. J., and Klumperman, J. (2001) *J. Cell Sci.* **114**, 3943–3952
22. Sachse, M., Urbe, S., Oorschot, V., Strous, G. J., and Klumperman, J. (2002) *Mol. Biol. Cell* **13**, 1313–1328
23. Yang, N., Huang, Y., Jiang, J., and Frank, S. J. (2004) *J. Biol. Chem.* **279**, 20898–20905
24. Lobie, P. E., Sadir, R., Graichen, R., Mertani, H. C., and Morel, G. (1999) *Exp. Cell Res.* **246**, 47–55
25. Govers, R., van Kerkhof, P., Schwartz, A. L., and Strous, G. J. (1997) *EMBO J.* **16**, 4851–4858
26. Strous, G. J., van Kerkhof, P., Govers, R., Ciechanover, A., and Schwartz, A. L. (1996) *EMBO J.* **15**, 3806–3812
27. Govers, R., ten Broeke, T., van Kerkhof, P., Schwartz, A. L., and Strous, G. J. (1999) *EMBO J.* **18**, 28–36
28. Greenhalgh, C. J., and Alexander, W. S. (2004) *Growth Horm. IGF Res.* **14**, 200–206
29. Yoshimura, A., Ohkubo, T., Kiguchi, T., Jenkins, N. A., Gilbert, D. J., Copeland, N. G., Hara, T., and Miyajima, A. (1995) *EMBO J.* **14**, 2816–2826
30. Ram, P. A., and Waxman, D. J. (2000) *J. Biol. Chem.* **275**, 39487–39496
31. Matsumoto, A., Masuhara, M., Mitsui, K., Yokouchi, M., Ohtsubo, M., Misawa, H., Miyajima, A., and Yoshimura, A. (1997) *Blood* **89**, 3148–3154
32. Gonzalez, L., Miquet, J. G., Sotelo, A. I., Bartke, A., and Turyn, D. (2002) *Endocrinology* **143**, 386–394
33. Miquet, J. G., Sotelo, A. I., Bartke, A., and Turyn, D. (2004) *Endocrinology* **145**, 2824–2832
34. Tollet-Egnell, P., Flores-Morales, A., Stavreus-Evers, A., Sahlin, L., and Norstedt, G. (1999) *Endocrinology* **140**, 3693–3704
35. Nicola, N. A., and Greenhalgh, C. J. (2000) *Exp. Hematol.* **28**, 1105–1112
36. Zhang, J. G., Farley, A., Nicholson, S. E., Willson, T. A., Zugaro, L. M., Simpson, R. J., Moritz, R. L., Cary, D., Richardson, R., Hausmann, G., Kile, B. J., Kent, S. B., Alexander, W. S., Metcalf, D., Hilton, D. J., Nicola, N. A., and Baca, M. (1999) *Proc. Natl. Acad. Sci. U. S. A.* **96**, 2071–2076
37. Verdier, F., Chretien, S., Muller, O., Varlet, P., Yoshimura, A., Gisselbrecht, S., Lacombe, C., and Mayeux, P. (1998) *J. Biol. Chem.* **273**, 28185–28190
38. Ram, P. A., and Waxman, D. J. (1999) *J. Biol. Chem.* **274**, 35553–35561
39. Du, L., Frick, G. P., Tai, L. R., Yoshimura, A., and Goodman, H. M. (2003) *Endocrinology* **144**, 868–876
40. Gebert, C. A., Park, S. H., and Waxman, D. J. (1997) *Mol. Endocrinol.* **11**, 400–414
41. Aman, M. J., Migone, T. S., Sasaki, A., Ascherman, D. P., Zhu, M., Soldaini, E., Imada, K., Miyajima, A., Yoshimura, A., and Leonard, W. J. (1999) *J. Biol. Chem.* **274**, 30266–30272
42. Moutoussamy, S., Renaudie, F., Lago, F., Kelly, P. A., and Finidori, J. (1998) *J. Biol. Chem.* **273**, 15906–15912
43. Masuhara, M., Sakamoto, H., Matsumoto, A., Suzuki, R., Yasukawa, H., Mitsui, K., Wakioka, T., Tanimura, S., Sasaki, A., Misawa, H., Yokouchi, M., Ohtsubo, M., and Yoshimura, A. (1997) *Biochem. Biophys. Res. Commun.* **239**, 439–446
44. Meng, L., Mohan, R., Kwok, B. H., Eloffson, M., Sin, N., and Crews, C. M. (1999) *Proc. Natl. Acad. Sci. U. S. A.* **96**, 10403–10408
45. Frick, G. P., Tai, L. R., and Goodman, H. M. (1994) *Endocrinology* **134**, 307–314
46. Wan, Y., Zheng, Y. Z., Harris, J. M., Brown, R., and Waters, M. J. (2003) *Mol. Endocrinol.* **17**, 2240–2250
47. Kempe, K. C., Isom, H. C., and Greene, F. E. (1995) *Biochem. Pharmacol.* **49**, 1091–1098
48. Laemmli, U. K. (1970) *Nature* **227**, 680–685
49. Park, S. H., Yamashita, H., Rui, H., and Waxman, D. J. (2001) *Mol. Endocrinol.* **15**, 2157–2171
50. Maley, F., Trimble, R. B., Tarentino, A. L., and Plummer, T. H., Jr. (1989) *Anal. Biochem.* **180**, 195–204
51. Moulin, S., Bouzinba-Segard, H., Kelly, P. A., and Finidori, J. (2003) *Cell. Signal.* **15**, 47–55
52. Gebert, C. A., Park, S. H., and Waxman, D. J. (1999) *Mol. Endocrinol.* **13**, 38–56
53. Adams, T. E., Hansen, J. A., Starr, R., Nicola, N. A., Hilton, D. J., and Billestrup, N. (1998) *J. Biol. Chem.* **273**, 1285–1287
54. Hansen, J. A., Lindberg, K., Hilton, D. J., Nielsen, J. H., and Billestrup, N. (1999) *Mol. Endocrinol.* **13**, 1832–1843
55. Silva, C. M., Day, R. N., Weber, M. J., and Thorner, M. O. (1993) *Endocrinology* **133**, 2307–2312
56. Zhang, Y., Jiang, J., Black, R. A., Baumann, G., and Frank, S. J. (2000) *Endocrinology* **141**, 4342–4348
57. Kamura, T., Sato, S., Haque, D., Liu, L., Kaelin, W. G., Jr., Conaway, R. C., and Conaway, J. W. (1998) *Genes Dev.* **12**, 3872–3881
58. Hanada, T., Yoshida, T., Kinjyo, I., Minoguchi, S., Yasukawa, H., Kato, S., Mimata, H., Nomura, Y., Seki, Y., Kubo, M., and Yoshimura, A. (2001) *J. Biol. Chem.* **276**, 40746–40754
59. Haan, S., Ferguson, P., Sommer, U., Hiremath, M., McVicar, D. W., Heinrich, P. C., Johnston, J. A., and Cacalano, N. A. (2003) *J. Biol. Chem.* **278**, 31972–31979
60. Ilangumaran, S., and Rottapel, R. (2003) *Immunol. Rev.* **192**, 196–211
61. Rui, L., Yuan, M., Frantz, D., Shoelson, S., and White, M. F. (2002) *J. Biol. Chem.* **277**, 42394–42398
62. Hicke, L., and Dunn, R. (2003) *Annu. Rev. Cell Dev. Biol.* **19**, 141–172
63. Kario, E., Marmor, M. D., Adamsky, K., Citri, A., Amit, I., Amariglio, N., Rechavi, G., and Yarden, Y. (2005) *J. Biol. Chem.* **280**, 7038–7048
64. Nicholson, S. E., Metcalf, D., Sprigg, N. S., Columbus, R., Walker, F., Silva, A., Cary, D., Willson, T. A., Zhang, J. G., Hilton, D. J., Alexander, W. S., and Nicola, N. A. (2005) *Proc. Natl. Acad. Sci. U. S. A.* **102**, 2328–2333
65. de Melker, A. A., van der Horst, G., and Borst, J. (2004) *J. Biol. Chem.* **279**, 55465–55473
66. Zhu, T., Goh, E. L., LeRoith, D., and Lobie, P. E. (1998) *J. Biol. Chem.* **273**, 33864–33875
67. Wang, L., Rudert, W. A., Loutaev, I., Roginskaya, V., and Corey, S. J. (2002) *Oncogene* **21**, 5346–5355
68. Blesofsky, W. A., Mowen, K., Arduini, R. M., Baker, D. P., Murphy, M. A., Bowtell, D. D., and David, M. (2001) *Oncogene* **20**, 7326–7333
69. Wakioka, T., Sasaki, A., Mitsui, K., Yokouchi, M., Inoue, A., Komiya, S., and Yoshimura, A. (1999) *Leukemia (Basel)* **13**, 760–767
70. Goh, E. L., Zhu, T., Leong, W. Y., and Lobie, P. E. (2002) *Endocrinology* **143**, 3590–3603
71. Takagi, K., Saito, Y., and Sawada, J. I. (2001) *Biol. Pharm. Bull.* **24**, 744–748
72. van Kerkhof, P., Smeets, M., and Strous, G. J. (2002) *Endocrinology* **143**, 1243–1252